Air-sea interactions in the Tropical Atlantic : a view based on lagged rotated maximum covariance analysis

Claude Frankignoul, Élodie Kestenare

Air–Sea Interactions in the Tropical Atlantic: A View Based on Lagged Rotated Maximum Covariance Analysis

CLAUDE FRANKIGNOUL

Université Pierre et Marie Curie, Institut Pierre-Simon Laplace, Laboratoire d'Océanographie Dynamique et de Climatologie, Paris, France

ELODIE KESTENARE

Laboratoire d'Etudes en Geophysique et Oceanographie Spatiales (LEGOS), CNES/CNRS/IRD/UPS 14, Toulouse, France

(Manuscript received 5 May 2004, in final form 10 March 2005)

ABSTRACT

The dominant air–sea feedbacks that are at play in the tropical Atlantic are revisited, using the 1958–2002 NCEP reanalysis. To separate between different modes of variability and distinguish between cause and effect, a lagged rotated maximum covariance analysis (MCA) of monthly sea surface temperature (SST), wind, and surface heat flux anomalies is performed. The dominant mode is the ENSO-like zonal equatorial SST mode, which has its maximum amplitude in boreal summer and is a strongly coupled ocean–atmosphere mode sustained by a positive feedback between wind and SST. The turbulent heat flux feedback is negative, except west of 25°W where it is positive, but countered by a negative radiative feedback associated with the meridional displacement of the ITCZ. As the maximum covariance patterns change little between lead and lag conditions, the in-phase covariability between SST and the atmosphere can be used to infer the atmospheric response to the SST anomaly. The second climate mode involves an SST anomaly in the tropical North Atlantic, which is primarily generated by the surface heat flux and, in boreal winter, wind changes off the coast of Africa. After it has been generated, the SST anomaly is sustained in the deep Tropics by the positive wind–evaporation–SST feedback linked to the wind response to the SST. However, north of about 10°N where the SST anomaly is largest, the wind response is weak and the heat flux feedback is negative, thus damping the SST anomaly. As the in-phase maximum covariance patterns primarily reflect the atmospheric forcing of the SST, simultaneous correlations cannot be used to describe the atmospheric response to the SST anomaly, except in the deep Tropics. Using instead the maximum covariance patterns when SST leads the atmosphere reconciles the results of recent atmospheric general circulation model experiments with the observations.

1. Introduction

The interannual variability of the tropical Atlantic is dominated by two modes: one is the Atlantic zonal equatorial mode that obeys similar dynamics to those of the El Niño–Southern Oscillation (ENSO) phenomenon. It involves sea surface temperature anomalies (SST) in the equatorial Atlantic, changes in the zonal slope of the equatorial thermocline, and anomalies in the Atlantic Walker and Hadley circulations, reaching maximum strength in boreal summer (e.g., Zebiak 1993; Carton and Huang 1994; Wang 2002). The other mode is an interannual to decadal fluctuation of the interhemispheric SST gradient that primarily involves SST variations in the tropical North Atlantic and is linked to north–south displacements of the intertropical convergence zone (ITCZ). It has often been referred to as "tropical Atlantic dipole," even though the anomalies in the North and South Tropical Atlantic are largely uncorrelated, as first shown by Houghton and Tourre (1992). The two modes are influenced by ENSO, either directly via changes in the Walker and Hadley circulations, or remotely via Rossby wave propagation through the extratropics. In particular, the tropical North Atlantic SST is directly affected in the spring following a mature phase of ENSO when the tropical

Corresponding author address: Claude Frankignoul, Université Pierre et Marie Curie, Institut Pierre-Simon Laplace, Laboratoire d'Océanographie Dynamique et de Climatologie, boîte 100, 4 place Jussieu, 75252 Paris Cedex 05, France.
E-mail: cf@lodyc.jussieu.fr

Pacific SST anomaly begins to weaken but anomalies in the far eastern equatorial Pacific are intensified, leading to a decrease in the northeast trade winds and the latent heat flux (e.g., Curtis and Hastenrath 1995; Enfield and Mayer 1997). The tropical North Atlantic SST is also forced by the North Atlantic Oscillation (NAO; e.g., Xie and Tanimoto 1998; Sutton et al. 2000; Czaja et al. 2002).

The Atlantic zonal equatorial mode involves a positive feedback between SST and the Walker cell, albeit weaker than in the ENSO phenomenon. During the warm SST phase, the trade winds relax, the thermocline is anomalously deep in the eastern basin, and the cold tongue of equatorial surface water does not appear, while convection is shifted southeastward. The lack of zonal SST gradient weakens the equatorial trade winds in the west, hence maintains the anomalous conditions. The wind thus acts as a positive feedback.

On the other hand, whether or not the meridional gradient mode is maintained by the positive wind–evaporation–SST (WES) feedback, as first suggested by Chang et al. (1997), remains controversial. The WES feedback is linked to the cross-equatorial surface wind induced by the interhemispheric SST gradient (wind toward the positive SST anomaly). The turning by the Coriolis force reduces the trade winds, hence the latent heat flux, in the hemisphere where SST is anomalously warm, which reinforces it (and conversely). Observational evidence derived from Comprehensive Ocean–Atmosphere Data Set (COADS) supporting the WES feedback was given in Chang et al. (2001), based in particular on the lagged correlation between the time series of the "dipole" mode of a maximum covariance analysis (hereafter MCA) between SST and three atmospheric variables (surface heat flux, zonal, and meridional wind). However, Frankignoul and Kestenare (2002, hereafter FK) found that the local heat flux feedback in the tropical Atlantic was primarily negative, and they suggested that Chang et al.'s (2001) positive feedback resulted in part from ENSO forcing and statistical degeneracy in the analysis. By separating the northern and southern parts of the domain in the lagged MCA, they removed the degeneracy and found that the net heat flux feedback was negligible on each part of the dipole, due to competing influence of a negative feedback over most of the region and a positive one near its western edge. This is consistent with the atmospheric general circulation model (AGCM) response studies discussed in Dommenget and Latif (2000) and Chang et al. (2000), except that in the latter the heat flux feedback was positive in a larger part of the western deep Tropics. Sutton et al. (2000) also found an anomalous cross-equatorial wind directed toward the positive SST anomaly, but the heat flux feedback was everywhere negative. Similarly, the cross-equatorial wind was strong in the AGCM experiments of Okumura et al. (2001), but the positive WES feedback was smaller than the negative feedback due to the temperature dependence of evaporation, so that it only reduced the SST anomaly damping. On the other hand, Ruiz-Barradas et al. (2003) found in a modeling study that the heat flux feedback was positive, except off northwest Africa. However, they used fluxes derived from the in-phase regression of atmospheric variables (air temperature and specific humidity) on the interhemispheric SST gradient, which may confuse cause and effect (Frankignoul 1999). As shown below, such confusion also explains the apparent discrepancy found by Wang and Carton (2003) between the latent heat flux feedback that they estimated from the COADS observations, which was positive, and that in six AGCMs, which was primarily negative in the tropical North Atlantic, and only positive (in most models) in the deep Tropics.

Since different AGCMs may behave differently, and different heat flux feedback strengths have been found in coupled models (Frankignoul et al. 2004), it is of interest to revisit the observations and clarify the nature of the air–sea coupling in the tropical Atlantic. In this paper, we focus on the atmospheric response to the main SST anomaly modes, which requires using multivariate analysis rather than a local approach. As statistical degeneracy prevented Frankignoul and Kestenare (2002) to successfully interpret the result of a lagged MCA in the whole tropical Atlantic domain, we use an extension of the method introduced by Cheng and Dunkerton (1995), who applied an orthogonal rotation to the spatial patterns derived from the MCA. Rotation emphasizes geographical regions characterized by the strongest relationships between two fields, so that the spatial patterns are more spatially localized, and the results easier to interpret. The results are also more robust. The extension is analogous to the varimax rotation commonly used in principal component analysis (Richman 1986), which successfully separates the northern and southern parts of the tropical Atlantic SST dipole that generally appear as a single empirical orthogonal pattern (EOF) in principal component analysis (e.g., Dommenget and Latif 2000).

The paper is organized as follows. The data are discussed in section 2. As in FK, the ENSO signal is removed prior to the analysis in order to single out the atmospheric response to the tropical Atlantic SST anomalies. The rotated MCA is described in section 3. It is applied to the relationship between SST, wind, and surface heat flux anomalies in section 4, where the two

main modes of variability are discussed. Their seasonal variability is discussed in section 5, and conclusions given in section 6.

2. The data

Because the COADS observations are noisy and sparse in the South Atlantic, we use the National Centers for Environmental Prediction–National Center for Atmospheric Research (NCEP–NCAR) reanalysis (Kalnay et al. 1996) that provides a more consistent dataset. The reanalysis is somewhat affected by model biases in the Tropics—in particular, for the surface heat fluxes. However, the time variability seems rather well represented and provides estimates of the local heat flux feedback that are broadly comparable to those derived from COADS, although there are small-scale discrepancies between the two datasets (FK; Frankignoul et al. 2004). Hence, even though the short-time variability of the turbulent heat flux may be poorly represented (Sun et al. 2003), the reanalysis may be used for our purposes. The MCA is based on monthly anomaly fields of SST, surface wind, and surface heat flux (positive downward), where the surface heat flux is the sum of the turbulent (latent plus sensible) and radiative (shortwave plus longwave) fluxes. To reduce the influence of trends and low-frequency changes, a third-order polynomial was removed from the monthly data by least squares fit. Since our estimation of the atmospheric feedback requires that the month-to-month intrinsic persistence of the atmospheric anomalies be small but ENSO teleconnections are persistent, we removed (some of) the ENSO influence by nonlinear seasonal regression analysis. ENSO was defined by the first two principal components of the detrended monthly SST anomalies in the tropical Pacific between 12.5°N and 12.5°S, which represent 78% of the variance in NCEP. Seasonally varying regression coefficients were determined by least squares fit for each variable and grid point, using successive sets of 3 months to get smoothly varying estimates. To take into account the phase asymmetry of the ENSO teleconnections, the regression was done separately for positive and negative values of the principal components. This straightforward nonlinear extension of the method used in FK seems well adapted since the ENSO teleconnection pattern changes between El Niño and La Niña conditions, but depends linearly on the tropical heating in the former case, and is independent of it in the latter one (Straus and Shukla 2002). The March regression was estimated from each February, March, and April (FMA), the April one from each March, April, and May (MAM), . . . As shown in Fig. 1 (top), the fractional variance linked to ENSO averages to less than 10% for the atmospheric fields and about 15% for SST, but it exceeds 20% at a few locations in the western tropical Atlantic. The amount of removed variance is generally small in summer and largest in late winter, exceeding 30% at time in the equatorial western Atlantic for zonal wind, north of South America for meridional wind, and in much of the tropical North Atlantic for SST, as illustrated in Fig. 1 (bottom).

It should be noted that we removed most of the direct, instantaneous (on monthly time scale) ENSO influence on each anomaly field, but not the delayed influence seen for example on SST during boreal spring (Enfield and Mayer 1997). However, the heat flux and wind anomalies in the tropical North Atlantic are best correlated with the simultaneous value of the ENSO index (Klein et al. 1999). Since our estimate of the atmospheric response to the tropical Atlantic SST anomalies—the main focus of this study—will be derived from the covariability between atmospheric and prior SST anomalies, it can be safely assumed that it is not significantly biased by ENSO. That the tropical Atlantic SST response to ENSO peaks after 4–5 months is irrelevant here.

3. Lagged rotated maximum covariance analysis

Lagged MCA has been increasingly used to determine the influence of the ocean on the atmosphere. Indeed, taking advantage of the separation between the time scale of the two media (outside the tropical Indo–Pacific), relationships between oceanic and atmospheric fields when the former leads by more than the atmospheric persistence are generally indicative of the influence of the ocean on the atmosphere, which is masked in phase or when the ocean follows by the larger impact of the atmosphere on the ocean (e.g., Czaja and Frankignoul 1999, 2002). As discussed in Bretherton et al. (1992) and Von Storch and Zwiers (1999), the MCA isolates pairs of spatial patterns and their associated time series by performing a singular value decomposition of the covariance matrix between two fields. Hence, an oceanic vector field $\mathbf{X}(t)$ at time t and an atmospheric one $\mathbf{Y}(t - \tau)$ at time $t - \tau$ are expanded into K orthogonal signals

$$\mathbf{X}(t) = \sum_{k=1}^{K} a_k(t)\mathbf{p}_k, \tag{1}$$

$$\mathbf{Y}(t - \tau) = \sum_{i=1}^{K} b_i(t - \tau)\mathbf{q}_i, \tag{2}$$

plus noise, with $\mathbf{p}_k \cdot \mathbf{p}_l = \delta_{kl}$, $\mathbf{q}_i \cdot \mathbf{q}_j = \delta_{ij}$, where the covariance between a_k and b_k is maximum for

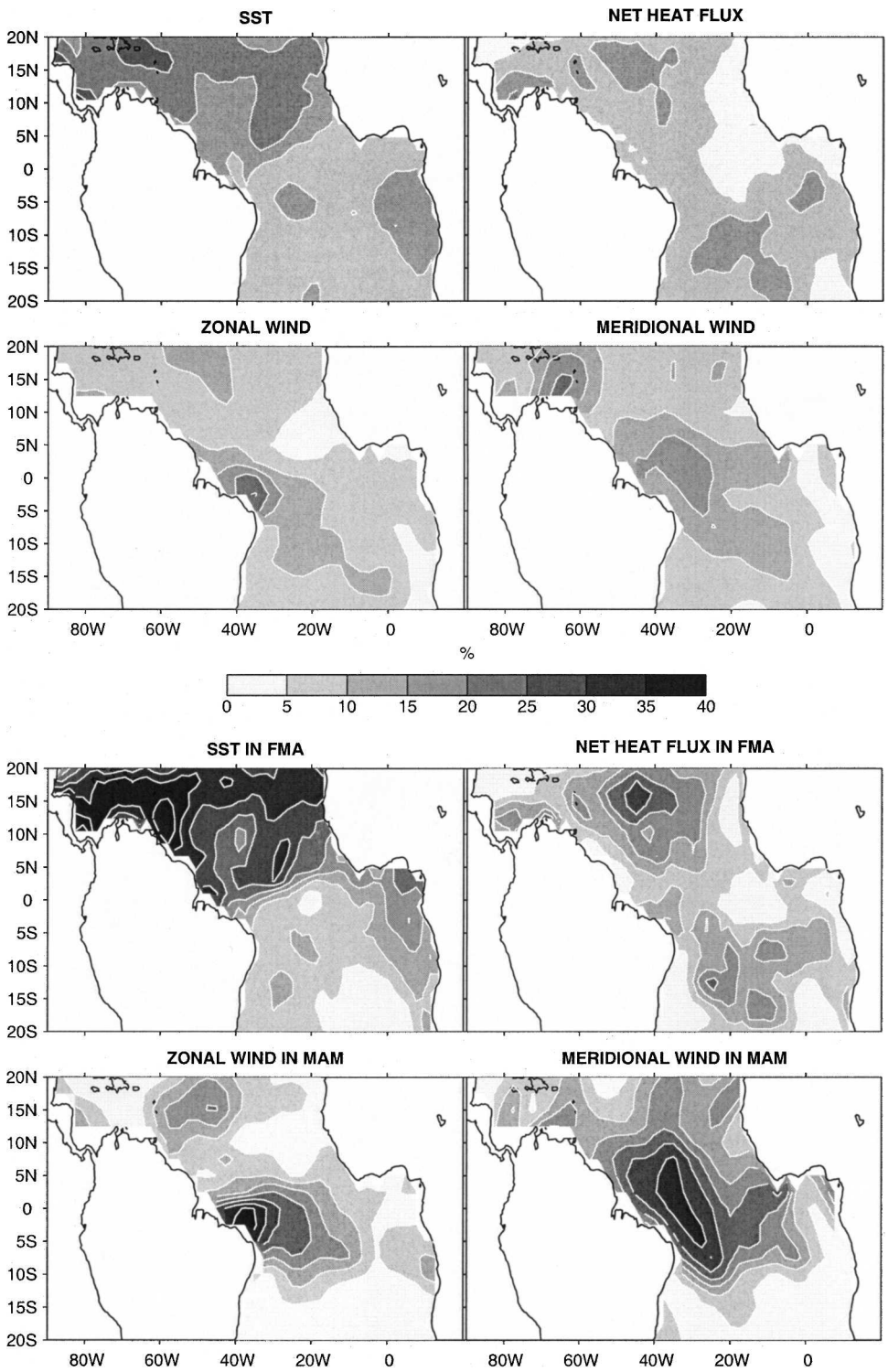

FIG. 1. (top four panels) Amount of fractional variance removed in association with ENSO for all months and (bottom four panels) in the season with peak values for each variable.

$k = 1, 2, \ldots$ and the time series are orthogonal to one another between the two fields, $\text{cov}(\mathbf{a}_k, \mathbf{b}_i) = \sigma_k \delta_{ki}$, which helps establishing one-to-one relationships. Here σ_k is the covariance explained by the pair of singular vectors $(\mathbf{p}_k, \mathbf{q}_k)$ and τ the time lag.

The MCA is a generalization of principal component analysis, reducing to it when the two fields are identical. In principal component analysis, spatial orthogonality can be a strong and undesirable constraint, in particular for limited samples in domains that are larger than the dominant spatial scale (like for SST anomalies in the tropical Atlantic), yielding patterns that may not correspond to physical modes. By relaxing the constraint of spatial orthogonality (hence, of variance maximization), linear rotation of a subset of leadings EOFs (usually by the varimax method) provides spatial patterns that are more geographically localized, and often more physically meaningful and statistically robust (Richman 1986; Cheng and Dunkerton 1995; Dommenget and Latif 2000). The constraint of maximum covariance in the MCA can lead to similar difficulties. An example is the Pan-Atlantic SST anomaly pattern discussed by Czaja and Frankignoul (2002) that preceded the winter NAO by a few months, but was shown in more local analyses to reflect the influence of two distinct SST anomalies, one in the midlatitudes and the other in the equatorial Atlantic.

As discussed by Cheng and Dunkerton (1995), pairs of patterns that are more geographically localized and easier to interpret can be obtained by applying a varimax orthogonal rotation to a subset of singular vectors, thereby creating spatial patterns that are no longer orthogonal within each field but tend to have a larger amplitude in the regions where the covariance between the two fields is large. The derivation of the rotated singular vector is described in Cheng and Dunkerton's excellent paper and it will not be repeated here, but note that the spatial patterns in (1) and (2) are no longer orthogonal after rotation. As for rotated EOFs, there is no obvious rule to determine the number of pairs of singular vectors to be retained in the rotation, except that it should be neither too small nor too large, and the rotated patterns should be stable within a fairly wide range of truncation points. In the present paper, the varimax rotation is performed using the first nine pairs of MCA modes that generally represented between 93% and 98% of the square covariance, depending on the lag. The results were largely insensitive to an increase in the number of pairs, but were sometimes harder to interpret with less than six pairs, suggesting that nine pairs is a reasonable choice.

Cheng and Dunkerton (1995) presented examples that illustrate the effectiveness of rotated MCA, but they only considered cases where the relationship between the two fields was very strong, as between sea level pressure and the 500-hPa height field. The relationship is much weaker in air–sea interaction studies when the ocean leads the atmosphere, so that careful statistical testing is first required to identify whether the coupled modes of variability can be considered to be meaningful. Statistical testing in MCA is generally based on a Monte Carlo method by comparing the estimated square covariance to that of a randomly scrambled ensemble. However, since rotation redistributes the covariance (and the square covariance) between the selected subset of pairs, the statistical testing must be done prior to rotation. As in Czaja and Frankignoul (2002), we used a moving blocks bootstrap approach (Von Storch and Zwiers 1999). Each MCA was repeated 100 times, linking the original SST anomalies with randomly scrambled atmospheric ones, so that the chronological order between the two fields was destroyed. To reduce the influence of serial correlation, blocks of two successive years were considered in the shuffling of the time sequence. Significance levels were estimated for the square covariance and the correlation by the percentage of randomized square covariance and correlation for the corresponding mode that exceeded the value being tested. Rotation was considered to be meaningful when the original MCA was statistically significant at the 10% level in both cases.

Below, we only discuss highly significant cases. We show homogeneous maps for the ocean and heterogeneous maps for the atmosphere [i.e., the projection of $\mathbf{X}(t)$ and $\mathbf{Y}(t - \tau)$ onto $a_k(t)$, referred to as maximum covariance patterns], since they preserve linear relations between the variables. This may not be the case for pairs of heterogeneous maps (Newman and Sardeshmukh 1994), although Cheng and Dunkerton (1995) showed that the linear relationship was largely recovered when using rotated patterns.

4. Air–sea interactions in the tropical Atlantic

The lagged MCA was first performed in the Atlantic domain between 20°N and 20°S separately for SST and surface heat flux anomalies, and for SST and surface wind anomalies. Since the results showed that, when statistically significant, the SST anomaly patterns in the first few modes were mostly very similar in the two cases, in particular after rotation, only the results of the MCA between SST anomalies and the combined fields of surface heat flux and wind anomalies will be displayed. The atmospheric fields were scaled to give equal weight to the heat flux and the wind in the analysis, and the results turned out to be even more signifi-

cant. To draw the figures, the time series were normalized so that the units of the maximum covariance patterns indicate typical magnitudes.

Between lag −5 (ocean leads) and 6 (ocean lags), the most persistent and significant covariability was found for the first two modes that were at least 10% significant (in both square covariance and correlation) at these lags. Mode 3 was also at least 10% significant between lag −4 and 5, and mode 4 between lag −3 and 6. As illustrated for the highly significant lag 0 in Fig. 2, the maximum covariance patterns often tend to cover the whole tropical Atlantic, presumably as a blend of different physical modes of variability, because of the constraint of spatial orthogonality. In particular, the SST dipole in mode 1 seems to combine the zonal equatorial mode and the meridional gradient mode, even though the two centers of action of the SST (as described by the two boxes 10°–20°N, 45°–10°W and 0°–10°S, 20°W–15°E) are uncorrelated. On the other hand, the SST monopole in mode 2 seems to extend the tropical North Atlantic SST anomalies to the whole domain. Mode 3 is a SST monopole in the tropical South Atlantic, and mode 4 is a coastal dipole whose centers of action of the SST (as described by 6°–15°N, 25°–10°W and 3°–20°S, 8°–15°E) are again uncorrelated. In addition, the lag dependence of the square covariance was not as well differentiated between modes as in the rotated analysis below. The rest of the paper is thus mostly based on the rotated MCA that gives more geographically confined patterns and more successfully separates the different SST modes. We mostly limit the discussion to the two dominant rotated modes of covariability since the third one is a subtropical South Atlantic mode with largest SST amplitude at the southern edge of the domain (as in Fig. 2, third panel), which should be investigated in a broader domain, and the coastal SST modes (in particular the southern pole in Fig. 2, bottom) were not robust and reflected little covariability between SST and the atmospheric fields.

a. The zonal equatorial SST mode

In the rotated MCA, the interaction between the zonal equatorial SST mode and the atmosphere, illustrated in its warm phase in Fig. 3, is the dominant MCA mode between lag −5 and 4, and it appears as one of the first two MCA modes at larger lags. Consistent with the atmosphere responding to the SST anomaly, the covariance and the correlation are maximum at zero lag, and they decrease slowly and nearly symmetrically at increasing positive or negative lags. The SST anomaly varies very little with lag and is largest along the equator, east of 20°W, and the southwestern African coast down to about 15°S. The SST amplitude is negligible in the northern Tropics, so that the dipole seen in Fig. 2 (top) has disappeared. The wind pattern (left) is rather broad, with winds that converge toward the warm SST along the equator and, in the Gulf of Guinea, slightly south of it, as predicted by the hydrostatic effect of SST on sea level pressure (Lindzen and Nigam 1987). The coupled pattern is consistent with the analysis of Servain et al. (1982) and Carton and Huang (1994), who showed that the anomalous equatorial westerlies to the west of the SST maximum accumulate warm water and deepen the thermocline in the eastern equatorial basin, thus preventing the appearance of the equatorial cold tongue. As the wind pattern also changes little with lag, the wind indeed acts as a dynamical positive feedback, and the mode is an ENSO-like, strongly coupled ocean–atmosphere mode.

The heat flux anomaly pattern (right) primarily shows a large heat loss above the warm SST anomaly, consistent with a negative heat flux feedback of 15–20 W m^{-2} K^{-1} (based on FK's method), but a weak heat gain (hence a positive feedback) west of 35°W. As shown by the regression on the lag-0 SST time series in Fig. 4, except near the equator the heat flux anomalies are dominated by the turbulent heat exchanges (mostly latent heat). East of 25°W, the turbulent heat flux feedback is negative and thus primarily associated with the thermodynamic cooling of the warm SST. In the western equatorial Atlantic, the latter seems to be dominated by the positive WES feedback caused by the decrease in the equatorial easterlies. There is also a radiative (short- and longwave) heat loss all along the equator, consistent with enhanced convection above warmer water, hence more high cirrus clouds and decreased incoming radiation, as during El Niño (Ramanathan and Collins 1991). In the western equatorial Atlantic, the negative radiative heat flux feedback strongly reduces or cancels the positive turbulent one, while in the Gulf of Guinea it enhances the negative feedback. These changes are associated with a southward shift of the ITCZ, as shown by the anomalous midtropospheric ascending motion on the southern side of the ITCZ climatological position, and descending motion to the north (Fig. 4, bottom).

The patterns are not significantly changed when the rotated MCA is done with wind or heat flux alone (not shown). The same symmetry in square covariance between positive and negative lags is found in the MCA between SST and wind, but the square covariance between SST and heat flux peaks at lag −1 and −2 (SST leads). This confirms that the two-way coupling mostly occurs via dynamical effects, while the heat flux primarily acts as a damping. The zonal mode is persis-

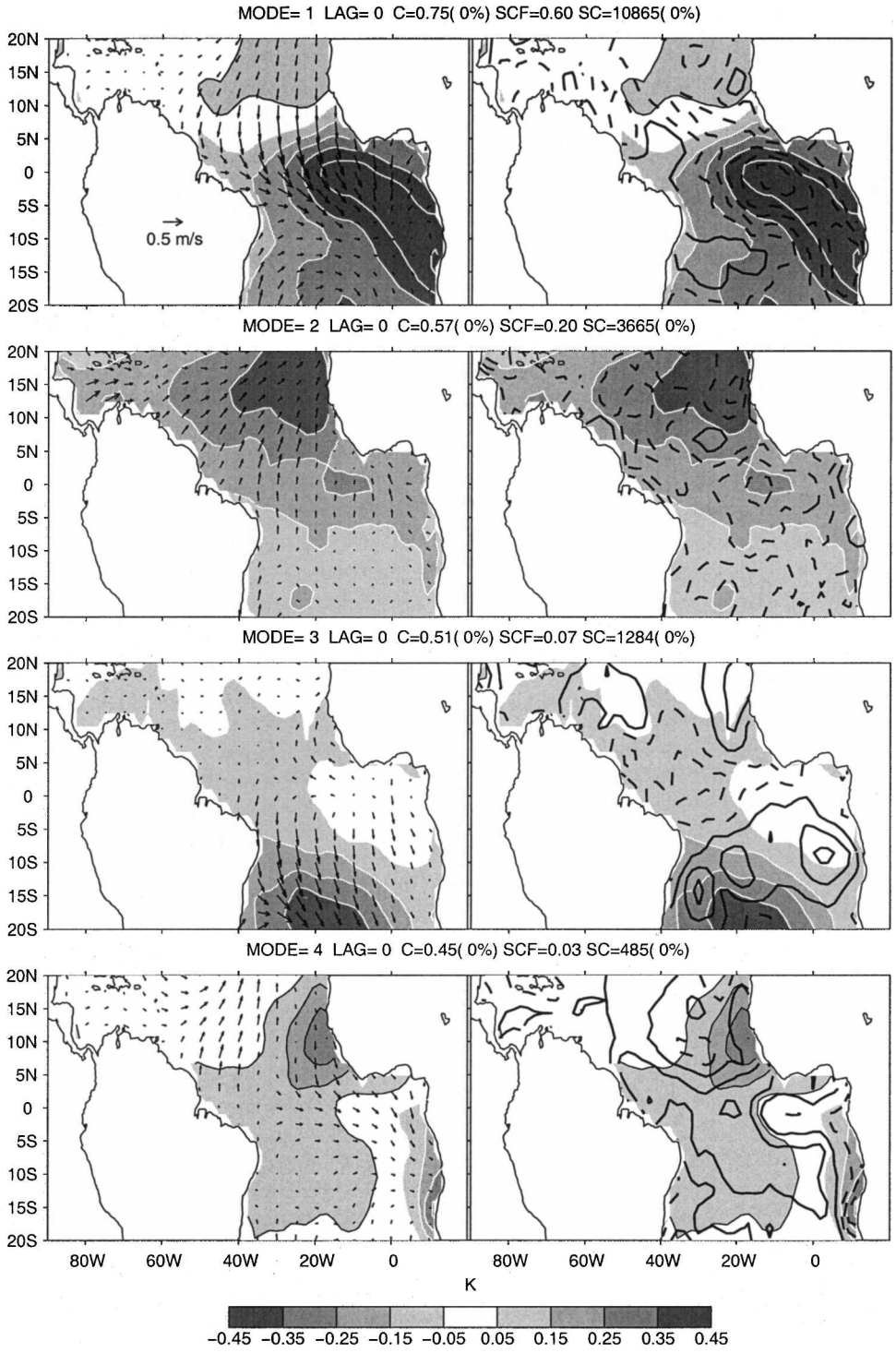

FIG. 2. First four MCA modes at lag 0 between SST (shading in K with white contours for positive values and black ones for negative value), (left) surface wind (scale given in the upper panel) and (right) surface heat flux anomalies (positive downward, contour interval = 2 W m^{-2} with negative values dashed). The time series are normalized so that the figures indicate typical magnitudes, C is the correlation between the two series, SC the square covariance, and SCF the SC fraction. Estimated statistical significance is given in parenthesis for C and SC.

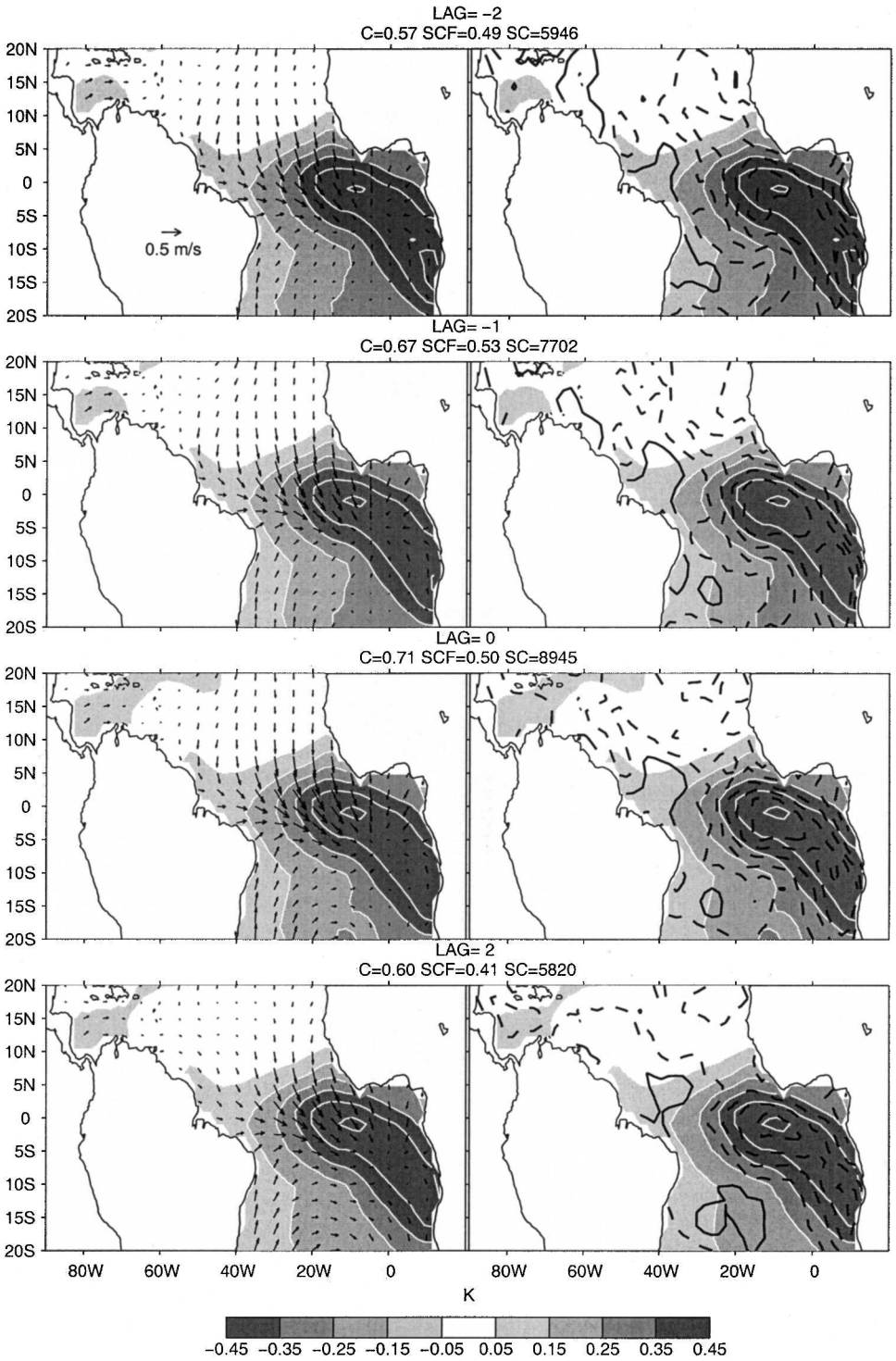

FIG. 3. As in Fig. 2 but for the first rotated MCA mode (the zonal equatorial mode) at lags −2, −1, 0, and 2. Ocean leads at negative lags (in months).

tent (Fig. 5), with an (approximate) *e*-folding time of 6 months, although the atmosphere also undergoes short time scale changes, as shown by the faster drop in the autocorrelations at lag 1.

In summary, the stability and symmetry of the rotated MCA in lead and lag conditions indicate that the wind and the heat flux primarily respond to the SST anomalies. Since the wind response sustains the oceanic

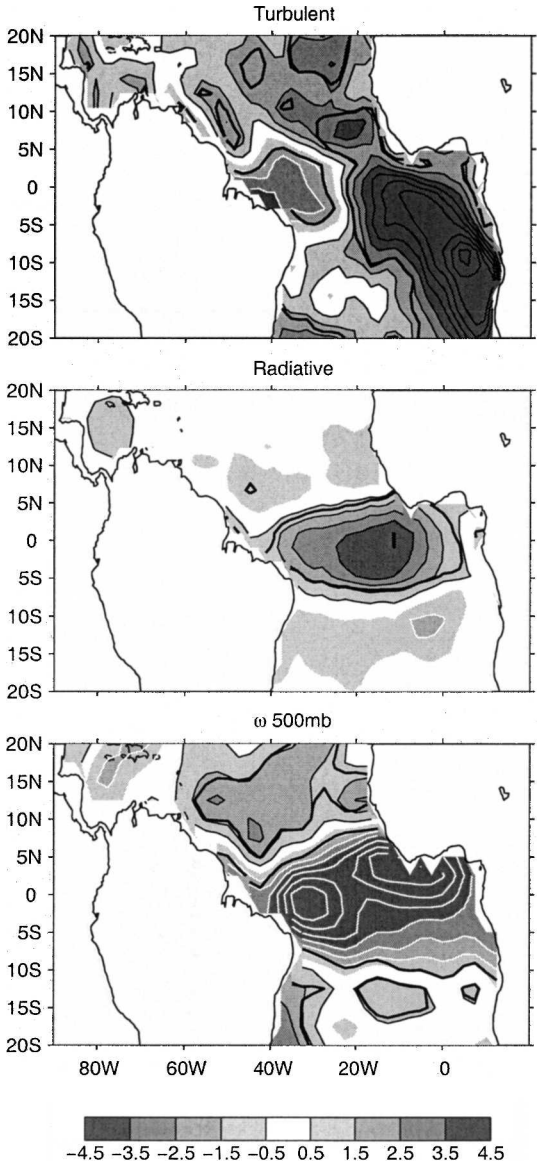

FIG. 4. Regression of anomalies in the (top) turbulent and (middle) radiative surface heat flux (positive downward, in W m^{-2}) and (bottom) the vertical velocity at 500 mb (positive upward, in 10^{-3} Pa s^{-1}) on the SST time series of the zonal equatorial mode at lag 0. White contours indicate positive values and black contours negative ones. The solid line indicates the 10% level of confidence.

processes that create the SST anomalies, the zonal equatorial SST mode is a truly coupled one where cause and effect are strongly linked, as in the ENSO. Inferences derived from simultaneous correlations between the ocean and the atmosphere thus represent well the atmospheric response to the SST, and our analysis confirms that given of Ruiz-Barradas et al. (2000) and Wang (2002), who in addition give a detailed description of the associated changes in the Walker and Hadley cells.

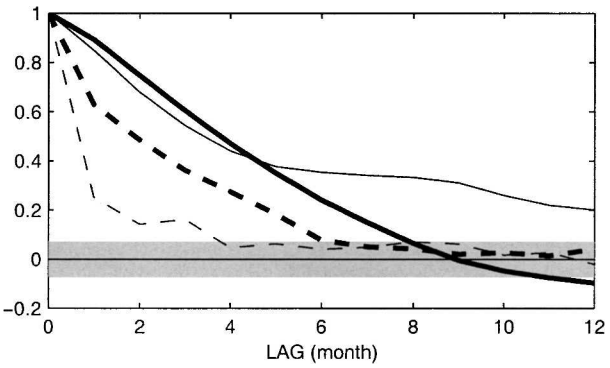

FIG. 5. Autocorrelation of the SST (continuous line) and atmospheric (dashed line) rotated MCA time series at lag 0 for mode 1 (thick) and 2 (thin).

b. *The tropical North Atlantic mode*

As in EOF analysis (Houghton and Tourre 1992; Dommenget and Latif 2000), the varimax rotation successfully separates the tropical North Atlantic SST anomalies from their equatorial/southern counterpart in the lagged MCA, consistent with their lack of linear correlation. The SST anomaly is maximum in the eastern tropical North Atlantic near 15°N, 25°W, and it resembles the northern part of the dipole of Curtis and Hastenrath (1995), Chang et al. (1997) and others, with only very small anomalies of the same sign south of the equator (Fig. 6). To distinguish it from the dipole, the mode is hereafter called the tropical North Atlantic SST mode, but note that the maximum SST gradient occurs near the mean position of the ITCZ, thus largely contributing to the variability of the interhemispheric temperature gradient. The mode appears as second rotated MCA mode between lag −1 and 4, and as second, third or fourth for larger negative lags (SST precedes), depending on the EOF truncation used in the varimax rotation, but as first for larger positive lags (SST follows), so that it tends to be more prominent when the atmosphere leads. The square covariance is large at lag 0 (although much smaller than for the zonal equatorial mode), peaks when SST follows by 1 month, and slowly decreases at larger positive lags, while at negative lags it decreases more rapidly. The (approximate) *e*-folding time of the tropical North Atlantic SST anomaly is comparable to that of the zonal mode, but it is more persistent at large lags (Fig. 5), reflecting both its larger decadal variability and the significant delayed ENSO influence. On the other hand, the persistence of the atmospheric maximum covariance pattern is short, al-

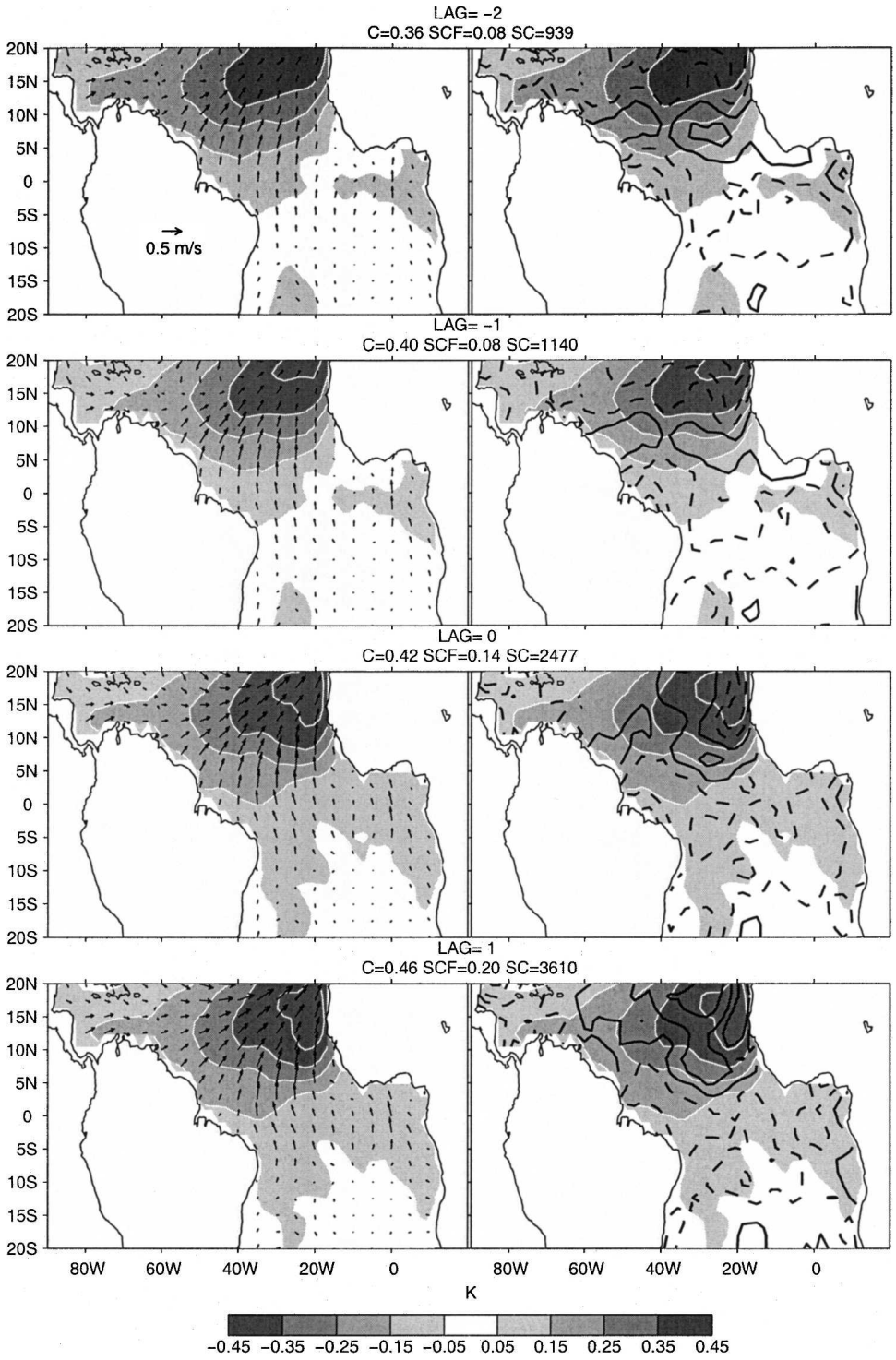

FIG. 6. As in Fig. 2 but for the tropical North Atlantic mode at lags −2, −1, 0, and 1, which corresponds to the second rotated MCA mode, except at lag −2 where it is the third one.

though there is also some variability on the long SST anomaly time scale. This temporal behavior is characteristic of SST anomalies that are primarily stochastically forced by the atmosphere, but also feedback onto it (Frankignoul 1985), consistent with the spatial patterns discussed below.

As illustrated in its positive phase in Fig. 6, the maximum covariance SST pattern only changes little with

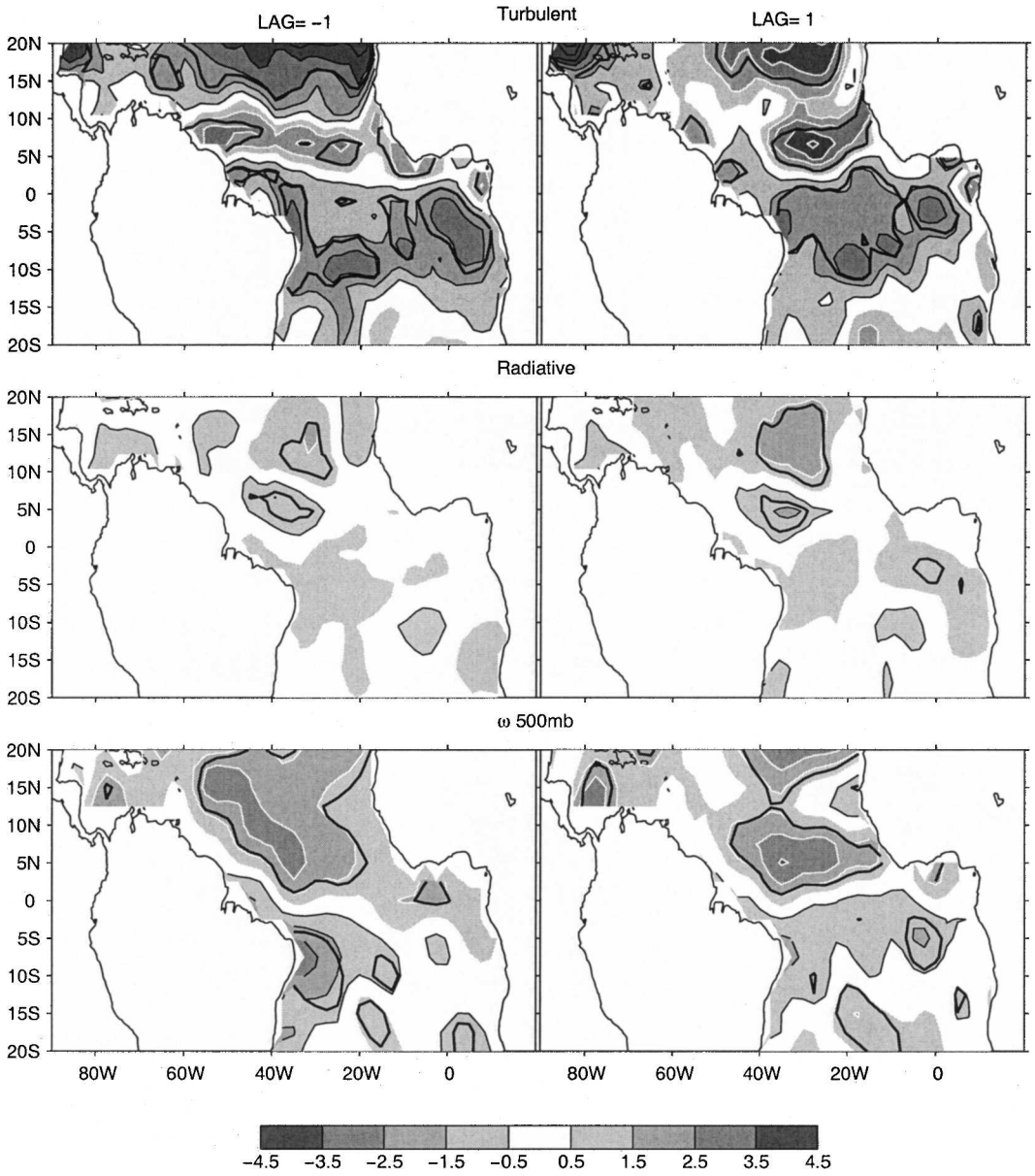

FIG. 7. As in Fig. 4 but for the tropical North Atlantic mode at lag (left) −1 and (right) 1.

lag (except off North Africa), while in the atmosphere there are important changes north of about 10°N. At positive lags when the atmosphere precedes, there is a strong weakening of the northeast trades in the northeastern part of the domain, together with nearly northward cross-equatorial winds but little signal south of 8°S. North of the equator, the surface heat flux anomaly into the ocean is positive and rather well collocated with the positive SST anomaly, confirming that the latter is primarily forced by heat flux anomalies, although coastal downwelling also plays an important role off Africa. Between the equator and 10°–15°S, there is a weak upward heat flux that should favor negative SST anomalies in the South Tropical Atlantic and thus an antisymmetric SST structure. However, the underlying SST anomaly is weakly positive instead, possibly because of compensating effect by ocean heat transport (Seager et al. 2001), or biases in the NCEP heat fluxes. As shown in Fig. 7 (right), the surface heat flux is strongly dominated by the turbulent fluxes and consistent with the decrease in the northeast trades, and it is only associated with weak vertical anomaly motions.

At negative lags when the ocean leads, the SST anomaly is similar, although the amplitude is reduced

off Africa south of 15°N. The wind anomaly pattern remains also similar, except that it is much weaker north of 10°N (Fig. 6). As shown by Joyce et al. (2004), the cross-equatorial winds drive a cross-equatorial Sverdrup transport in the ocean away from the warm side of the equator, thus opposite the winds. At the same time, the heat flux anomaly north of about 10°N changes of sign between positive and negative lags: it is negative when SST precedes, thereby damping (existing) SST anomalies, most strongly so in the northeastern corner where the SST amplitude is large. On the other hand, the surface heat flux anomaly does not change sign between about 3° and 10°N, thus acting as a positive feedback on existing SST anomalies. Since the wind anomaly in this narrow latitude band is large and oriented toward the warm SST anomaly, the trade winds are weaker than normal and the heat flux consistent with the WES feedback, while farther north the heat flux feedback is dominated by the thermodynamics. Figure 7 shows that the heat flux feedback is primarily due to the turbulent fluxes, although around 5°N, 40°W it is to a small extent offset by the radiation flux. North of the equator, the latter shows hint of a meridional dipole that would be consistent with the cloud changes discussed by Tanimoto and Xie (2002). Near and south of the equator, the heat flux anomaly remains of the same sign as at positive lags, so that it should damp the very weak SST anomalies that are seen there in Fig. 6. In summary, the heat flux feedback associated with the tropical North Atlantic SST mode is negative north of 10°N but positive in the deep Tropics. This is consistent with FK and Czaja et al. (2002), although in COADS (FK) the positive heat flux feedback was located more on the western side of the tropical North Atlantic (but note that small-scale features in the NCEP heat fluxes anomalies may not be reliable). By damping the SST anomaly to the north and enhancing it to the south, the heat flux feedback should also act as a southward propagator. Figure 7 (bottom) shows that the positive tropical North Atlantic SST creates ascending motions north of the equator and descending ones on the western side of the Tropical South Atlantic, consistent with the northward shift of the ITCZ described e.g., in Ruiz-Barradas et al. (2000) and Wang (2002).

As discussed in Frankignoul et al. (1998) and Frankignoul (1999), the simultaneous covariability (lag 0) can be dominated either by the atmospheric forcing of the ocean or the oceanic forcing of the atmosphere, depending on the relative strength of the interactions, and it should be interpreted with care. Figure 6 shows that at lag 0 the atmospheric maximum covariance patterns closely resemble those found at positive lags when SST follows, except off North Africa where the heat flux forcing is weak and thus does not mask the heat flux tendency to damp existing SST anomalies. Hence, the lag-0 patterns mainly reflect the atmospheric forcing of the SST, *not the atmospheric response to the SST* as often assumed. Because the wind and heat flux patterns change little in the deep Tropics between lead and lag conditions, interpreting the in-phase patterns as the atmospheric response to the tropical North Atlantic SST mode is of no consequence in this region. However, it leads to erroneous conclusions north of about 10°N, where the SST anomaly is large, as it would do at higher latitudes. Interestingly, our estimate of the heat flux feedback (i.e., that based on negative lags) is in good agreement with the response of most atmospheric GCMs discussed by Wang and Carton (2003).

5. Seasonal variability

Since the main SST modes undergo strong seasonal variations, the MCA and the rotated MCA were also done seasonally by binning the monthly anomalies into groups of 3 successive months, as in Czaja and Frankignoul (2002). For instance, for boreal summer the atmospheric fields in June–July–August (JJA) were compared for each year with the JJA SST at lag 0, the JAS SST at lag 1, and so on. Since the sample is smaller, the results are slightly noisier, but they document well the seasonal modulation of the coupled modes.

As discussed before, the zonal equatorial SST mode is strongly linked to the seasonal cycle since a warm event occurs when the boreal summer uplifting of the thermocline in the eastern equatorial Atlantic does not occur, preventing the appearance of the cold SST tongue (Carton and Huang 1994). Correspondingly, the zonal equatorial mode was prevalent in the rotated MCA when SST was taken between late spring (AMJ) and early winter (NDJ), with maximum covariance in JJA. Note that rotation primarily acted by suppressing or strongly reducing the strong MCA tendency in late spring and early summer (but not later until fall) to have as first two SST modes a dipole and a monopole. This is illustrated for AMJ in Fig. 8 (top two panels), where the dipole–monopole tendency is much stronger than when all months were included (see Fig. 2). Nonetheless, rotation singles out the zonal SST mode (third panel) and the tropical North Atlantic mode (bottom panel). As shown by the similarity with Fig. 3, the maximum covariance patterns for the zonal mode suggest similar air–sea coupling as on an annual basis. Between midsummer and early winter, the standard MCA primarily shows SST monopoles as first two modes, with centers of action corresponding to those of the zonal

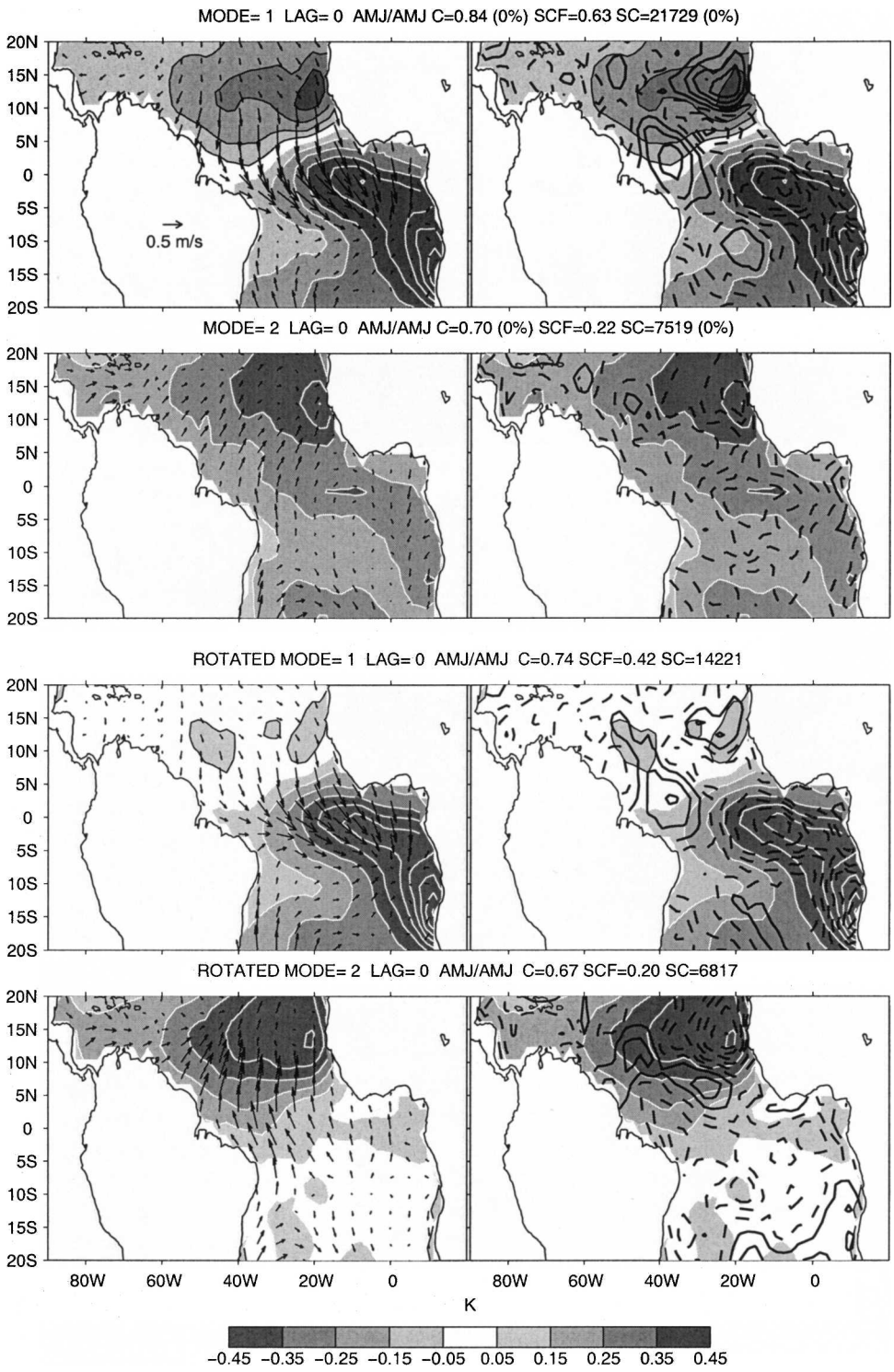

FIG. 8. (top two panels) First and second MCA modes at lag 0 between SST (shading in K with white contours for positive values and black ones for negative value), (left) surface wind (scale given in the upper panel), and (right) surface heat flux (positive downward, contour interval = 2 W m^{-2} with negative values dashed) anomalies in AMJ. (bottom two panels) As above, but for the first two rotated MCA modes.

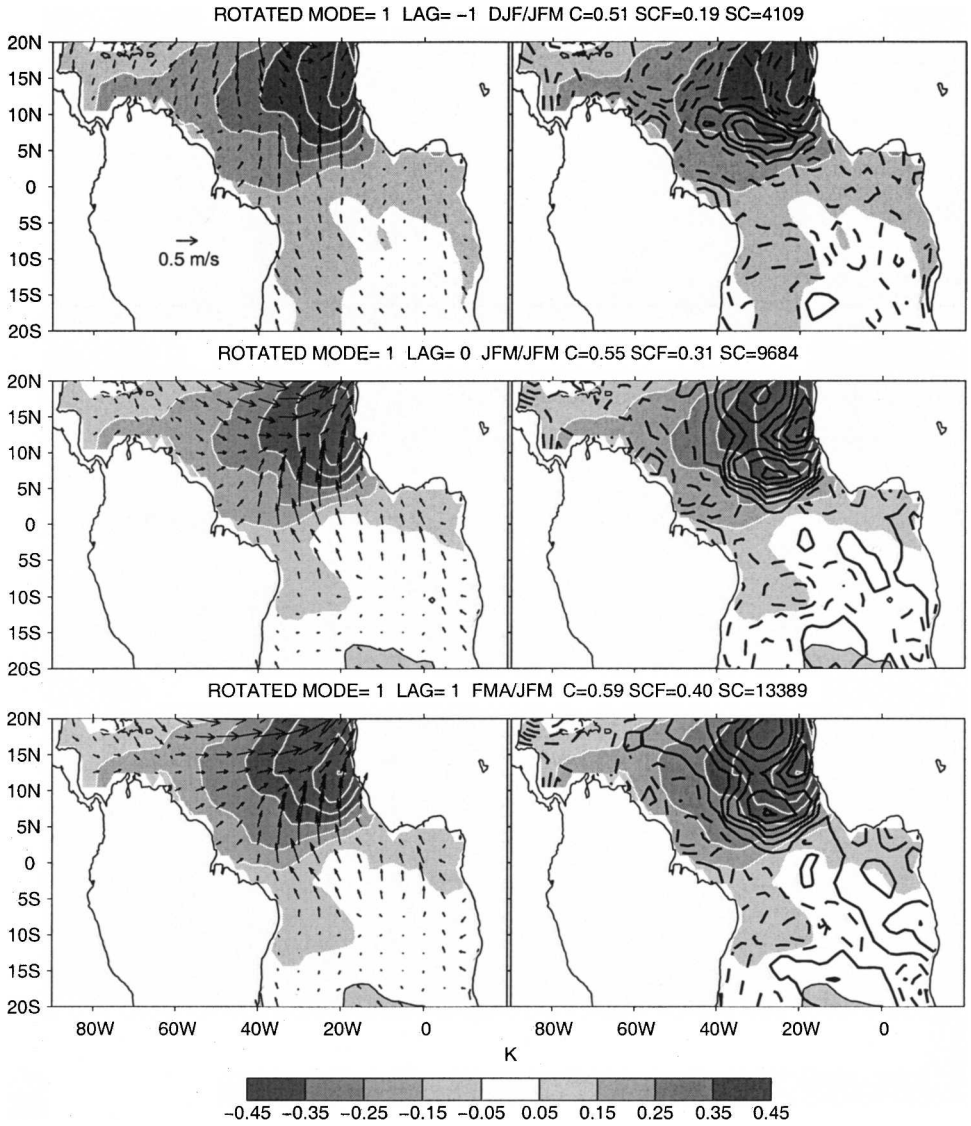

FIG. 9. As in Fig. 8, but for the first rotated MCA mode at lags (top) −1, (middle) 0, and (bottom) 1 when the atmosphere is taken in JFM and SST in DJF, JFM, and FMA, respectively.

and the tropical North Atlantic SST modes, respectively. Rotation then plays a lesser role but contributes to having more geographically localized modes (not shown).

From midwinter to midspring, the MCA again tends to produce SST dipoles and monopoles in the first two modes (not shown), but rotation suppresses the dipole tendency. In this period, the first rotated MCA mode becomes the tropical North Atlantic mode, with maximum covariance in JFM, while the South Tropical Atlantic mode competes with the zonal equatorial mode and the southern coastal mode as second or third rotated mode. The MCA for the tropical North Atlantic mode is illustrated in Fig. 9 for the atmosphere in JFM and SST one month earlier (top), in phase (middle), or one month after (bottom). Lag 1 confirms that the tropical North Atlantic mode is primarily forced by the surface heat exchanges and, off North Africa, the wind that counters the coastal upwelling prevailing in boreal winter. Projecting the anomaly fields north of 20°N onto the MCA time series shows that in this season the tropical North Atlantic mode is closely linked to the NAO: the SST anomaly is the southern pole of the North Atlantic SST anomaly tripole, and the atmospheric forcing is that associated with the NAO (not shown). At lag 0, the atmospheric maximum covariance patterns resemble those at positive lags and thus mostly reflect the atmospheric forcing, as in the annual case.

Lag −1, on the other hand, reflects the SST influence on the atmospheric circulation. It shows again little changes south of 10°N (hence a positive feedback in the deep Tropics), but weaker winds and a sign reversal in the heat flux north of 10°N (hence a negative heat flux feedback). At lag −1, there is very little association with the North Atlantic SST anomaly tripole, and none with the NAO. Later in spring, the atmospheric forcing of the mode weakens, and the MCA then primarily reflects the atmospheric response to the existing SST anomaly, as was seen in late spring for the second mode at lag 0 (Fig. 8, bottom panel). The seasonal modulation of the atmospheric forcing thus needs to be considered when interpreting seasonal data.

6. Summary and conclusions

To investigate the main air–sea feedbacks in the tropical Atlantic, we have used a lagged rotated MCA of SST, wind, and surface heat flux anomalies in the NCEP reanalysis. Standard MCA has a tendency to often produce artificial SST dipole and monopole as first MCA modes, and it was the case for the Tropical Atlantic. Just as in the case of EOF analysis, varimax rotation suppressed this tendency, and it successfully separated (on both annual and seasonal basis, and even when using yearly averages) the two main modes of tropical Atlantic variability, namely the zonal equatorial SST mode and the tropical North Atlantic SST mode that were linked in the standard MCA. This is consistent with the lack of correlation of their centers of action. In addition, after rotation the two modes had a more distinct behavior in lead and lag conditions, and the basic difference between the deep Tropics, where the WES feedback is strong, and the higher tropical latitudes, where it is weak, appeared more clearly. Rotated MCA thus retains its effectiveness when the covariability between the fields is not strong, and its use can be recommended for air–sea interaction studies.

The main mode is the ENSO-like zonal equatorial SST mode, which is a strongly coupled ocean–atmosphere mode sustained by a positive feedback between wind and SST. In its positive phase, wind anomalies converge toward the warm SST along the equator and, in the Gulf of Guinea, south of it, consistent with the sea level pressure response to the SST anomaly (Lindzen and Nigam 1987), so that the anomalous equatorial westerlies to the west accumulate warm water and deepen the thermocline in the east, thus preventing the spring appearance of the cold tongue (Carton and Huang 1994). The heat flux feedback is negative and primarily due to the turbulent fluxes, although west of 25°W the turbulent heat flux feedback is positive, consistent with the WES mechanism. However, it is largely compensated by the negative radiative feedback that is associated with the southward shift of the ITCZ. As the maximum covariance patterns change little between lead and lag conditions, the in-phase covariability between SST and the atmosphere can be used to infer the atmospheric response to the SST anomaly, as in Ruiz-Barradas et al. (2000, 2003) and Wang (2002).

The second rotated MCA mode is the tropical North Atlantic SST mode (also called interhemispheric SST gradient mode), which is a weakly coupled ocean–atmosphere mode where the SST anomaly is primarily generated by changes in the surface heat flux and, in boreal winter, the wind off the coast of Africa. After it has been generated, the SST anomaly has a strong influence on the wind in the deep Tropics, but a small one farther north. Hence, the SST anomaly is sustained by the positive WES feedback in the deep Tropics, but north of 10°N where the SST amplitude is largest, thermodynamics prevail and the heat flux feedback is negative, thus damping the SST anomaly. As the in-phase maximum covariance patterns primarily reflect the atmospheric forcing of the SST, simultaneous correlations cannot be used everywhere to describe the atmospheric response to the SST anomaly. In particular, results based on simultaneous correlations as in Ruiz-Barradas et al. (2000, 2003), Tanimoto and Xie (2002), and others reflect north of 10°N the atmospheric forcing of the SST, not its response, and Wang and Carton's (2003) conclusion that GCMs fail to reproduce the WES feedback primarily results from confusing cause and effect in the observations, not from model deficiencies.

It should be noted that the rotated MCA clearly separated the tropical North Atlantic mode not only from the zonal equatorial mode but also from the South Tropical Atlantic mode. This also held when the analysis was based on yearly means rather than monthly ones. However, no attempt was made to consider longer time scales as the sample would be too small to perform the rotated MCA confidently.

In this analysis, the direct ENSO influence on the tropical Atlantic fields was first removed from the monthly anomaly data. Because our main focus was on the air–sea feedback, this was a necessary first step since, as discussed in FK, the persistence of the ENSO teleconnections biases the estimates of the atmospheric response that are based on lagged correlations. However, it should be recalled that ENSO largely contributes to the tropical Atlantic variability (e.g., Curtis and Hastenrath 1995; Enfield and Mayer 1997). Retaining the ENSO signal in the rotated MCA had a negligible

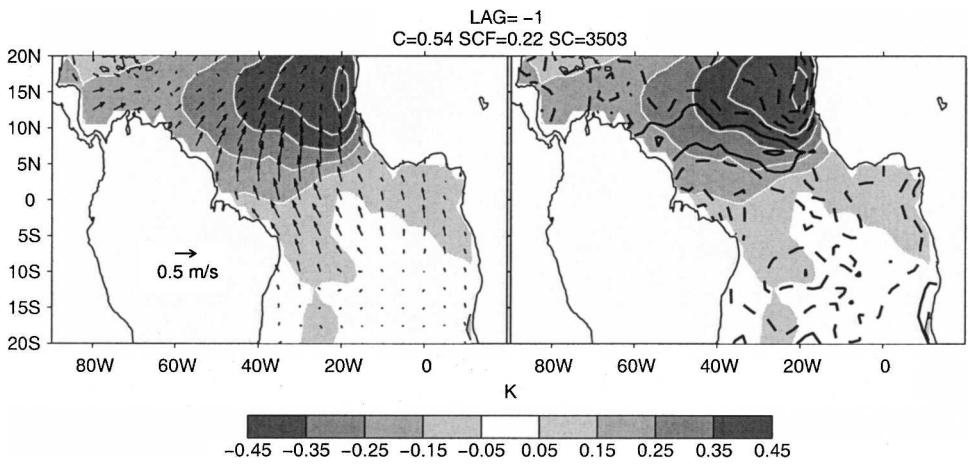

FIG. 10. As in Fig. 6 at lag −1, but without removing the ENSO teleconnections.

impact on the zonal equatorial mode and the Tropical South Atlantic mode. However, it strongly affected the tropical North Atlantic mode, enhancing the square covariance by nearly a factor 2 at lag ≥ 0, consistent with Czaja et al. (2002), and by more than a factor 2 at lag <0, albeit with little change in pattern except for stronger cross-equatorial winds. This is illustrated in Fig. 10, which should be compared with Fig. 6, second panel. Thus, the ENSO signal must be removed when investigating the air–sea feedback associated with the interhemispheric SST gradient.

Finally, a word of caution is needed since we used the NCEP reanalysis, not direct observations. Although the heat flux feedback was found to be fairly comparable in NCEP and COADS (FK; Frankignoul et al. 2004), model biases and inadequate bulk algorithms may affect our results, which should be verified when improved data become available.

Acknowledgments. We thank N. Sennéchael for her help. The NCAR–NCEP Reanalysis data was provided through the NOAA Climate Center (online at http://www.cdc.noaa.gov/). Support from the Institut universitaire de France is gratefully acknowledged.

REFERENCES

Bretherton, C. S., C. Smith, and J. M. Wallace, 1992: An intercomparison of methods for finding coupled patterns in climate data. *J. Climate,* **5,** 541–560.

Carton, J. A., and B. Huang, 1994: Warm events in the Tropical Atlantic. *J. Phys. Oceanogr.,* **24,** 888–902.

Chang, P., L. Ji, and H. Li, 1997: A decadal climate variation in the tropical Atlantic Ocean from thermodynamic air-sea interactions. *Nature,* **385,** 516–518.

——, R. Saravanan, J. Link, and G. C. Hegerl, 2000: The effect of local sea surface temperatures on atmospheric circulation over the tropical Atlantic sector. *J. Climate,* **13,** 2195–2216.

——, L. Ji, and R. Saravanan, 2001: A hybrid coupled model study of tropical Atlantic variability. *J. Climate,* **14,** 361–390.

Cheng, X., and T. J. Dunkerton, 1995: Orthogonal rotation of spatial patterns derived from singular value decomposition analysis. *J. Climate,* **8,** 2631–2643.

Curtis, S., and S. Hastenrath, 1995: Forcing of anomalous sea surface temperature evolution in the tropical Atlantic during Pacific warm events. *J. Geophys. Res.,* **100,** 15 835–15 847.

Czaja, A., and C. Frankignoul, 1999: Influence of the North Atlantic SST on the atmospheric circulation. *Geophys. Res. Lett.,* **26,** 2969–2972.

——, and ——, 2002: Observed impact of Atlantic SST anomalies on the North Atlantic oscillation. *J. Climate,* **15,** 606–623.

——, P. van der Vaart, and J. Marshall, 2002: A diagnostic study of the role of remote forcing in tropical Atlantic variability. *J. Climate,* **15,** 3280–3290.

Dommenget, D., and M. Latif, 2000: Interannual to decadal variability in the tropical Atlantic. *J. Climate,* **13,** 777–792.

Enfield, D. B., and D. A. Mayer, 1997: Tropical Atlantic sea surface temperature variability and its relation to El Niño-Southern Oscillation. *J. Geophys. Res.,* **102,** 929–945.

Frankignoul, C., 1985: Sea surface temperature anomalies, planetary waves and air-sea feedback in the middle latitudes. *Rev. Geophys.,* **23,** 357–390.

——, 1999: A cautionary note on the use of statistical atmospheric models in the middle latitudes: Comments on "Decadal variability in the North Pacific as simulated by a hybrid coupled model." *J. Climate,* **12,** 1871–1872.

——, and E. Kestenare, 2002: The surface heat flux feedback. Part I: Estimates from observations in the Atlantic and the North Pacific. *Climate Dyn.,* **19,** 633–647.

——, A. Czaja, and B. L'Heveder, 1998: Air-sea feedback in the North Atlantic and surface boundary conditions for ocean models. *J. Climate,* **11,** 2310–2324.

——, E. Kestenare, M. Botzet, A. F. Carril, H. Drange, A. Pardaens, L. Terray, and R. Sutton, 2004: An intercomparison between the surface heat flux feedback in five coupled models, COADS and the NCEP reanalysis. *Climate Dyn.,* **22,** 373–388.

Houghton, R. W., and Y. Tourre, 1992: Characteristics of low frequency sea surface temperature fluctuations in the tropical Atlantic. *J. Climate,* **5,** 765–771.

Joyce, T. M., C. Frankignoul, Y. Yang, and H. E. Phillips, 2004: Ocean response and feedback to the SST dipole in the tropical Atlantic. *J. Phys. Oceanogr.,* **34,** 2525–2540.

Kalnay, E., and Coauthors, 1996: The NCEP/NCAR 40-Year Reanalysis Project. *Bull. Amer. Meteor. Soc.,* **77,** 437–471.

Klein, S. A., B. J. Soden, and N. C. Lau, 1999: Remote sea surface temperature variations during ENSO: Evidence for a tropical atmospheric bridge. *J. Climate,* **12,** 917–932.

Lindzen, R. S., and S. Nigam, 1987: On the role of sea-surface temperature gradients in forcing low-level winds and convergence in the Tropics. *J. Atmos. Sci.,* **44,** 2418–2436.

Newman, M., and P. D. Sardeshmukh, 1994: A caveat concerning singular value decomposition. *J. Climate,* **8,** 352–360.

Okumura, Y., S. P. Xie, A. Numaguti, and Y. Tanimoto, 2001: Tropical Atlantic air-sea interaction and its influence on the NAO. *Geophys. Res. Lett.,* **28,** 1507–1510.

Ramanathan, V., and W. Collins, 1991: Thermodynamic regulation of ocean warming by cirrus clouds deduced from observations of the 1987 El Niño. *Nature,* **13,** 325–347.

Richman, M. B., 1986: Rotation of principal components. *J. Climatol.,* **6,** 293–335.

Ruiz-Barradas, A., J. A. Carton, and S. Nigam, 2000: Structure of interannual-to-decadal climate variability in the Tropical Atlantic sector. *J. Climate,* **13,** 3285–3297.

——, ——, and ——, 2003: Role of the atmosphere in climate variability of the Tropical Atlantic. *J. Climate,* **16,** 2053–2065.

Seager, R., Y. Kushnir, P. Chang, N. Naik, J. Miller, and W. Hazeleger, 2001: Looking for the role of the ocean in tropical Atlantic decadal climate variability. *J. Climate,* **14,** 638–655.

Servain, J., J. Picaut, and J. Merle, 1982: Evidence of remote forcing in the equatorial Atlantic Ocean. *J. Phys. Oceanogr.,* **12,** 457–463.

Straus, D. M., and J. Shukla, 2002: Does ENSO force the PNA? *J. Climate,* **15,** 2340–2358.

Sun, B., L. Yu, and R. A. Weller, 2003: Comparisons of surface meteorology and turbulent heat fluxes over the Atlantic: NWP model analysis versus moored buoy observations. *J. Climate,* **16,** 679–695.

Sutton, R. T., S. P. Jewson, and D. P. Rowell, 2000: The elements of climate variability in the tropical Atlantic region. *J. Climate,* **13,** 3261–3284.

Tanimoto, Y., and S. P. Xie, 2002: Interhemispheric decadal variations in SST, surface wind, heat flux and cloud cover over the Atlantic ocean. *J. Meteor. Soc. Japan,* **80,** 1199–1219.

Von Storch, H., and F. W. Zwiers, 1999: *Statistical Analysis in Climate Research.* Cambridge University Press, 342 pp.

Wang, C., 2002: Atlantic climate variability and its associated atmospheric circulation cells. *J. Climate,* **15,** 1516–1536.

Wang, J., and J. Carton, 2003: Modeling climate variability in the Tropical Atlantic atmosphere. *J. Climate,* **16,** 3858–3876.

Xie, S. P., and Y. Tanimoto, 1998: A pan-Atlantic decadal climate oscillation. *Geophys. Res. Lett.,* **25,** 2185–2188.

Zebiak, S. E., 1993: Air-sea interaction in the equatorial Atlantic region. *J. Climate,* **6,** 1567–1586.